Article:

Al-Saffar, A. and Kim, E. (2017) Sustainable theory of a logistic model - Fisher Information approach. Mathematical Biosciences, 285. pp. 81-91. ISSN 0025-5564

https://doi.org/10.1016/j.mbs.2016.12.009

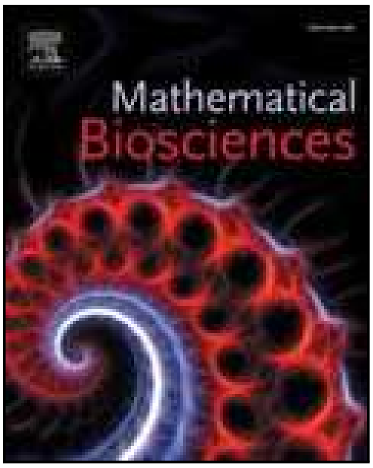

Sustainable theory of a logistic model - Fisher Information approach

Avan Al-Saffar, Eun-jin Kim

PII: S0025-5564(16)30420-5
DOI: 10.1016/j.mbs.2016.12.009
Reference: MBS 7897

To appear in: *Mathematical Biosciences*

Received date: 26 April 2016
Revised date: 29 December 2016
Accepted date: 31 December 2016

Please cite this article as: Avan Al-Saffar, Eun-jin Kim, Sustainable theory of a logistic model - Fisher Information approach, *Mathematical Biosciences* (2017), doi: 10.1016/j.mbs.2016.12.009

Highlights

- Logistic model's sustainability for perturbation in positive and/or negative feedback
- Maintenance of a long-term memory of initial conditions and distinct bimodal dist.
- Utility of Fisher information (FI) as a useful measure of sustainability.
- Optimal FI and its relation to the robustness against different perturbation.

Sustainable theory of a logistic model - Fisher Information approach

Avan Al-Saffar[a] and Eun-jin Kim[a]
[a] School of Mathematics and Statistics, The University of Sheffield, Sheffield, South Yorkshire S3 7RH, UK.
E-mail: asal-saffar1@sheffield.ac.uk and e.kim@sheffield.ac.uk

Abstract. Information theory provides a useful tool to understand the evolution of complex nonlinear systems and their sustainability. In particular, Fisher information has been evoked as a useful measure of sustainability and the variability of dynamical systems including self-organising systems. By utilising Fisher information, we investigate the sustainability of the logistic model for different perturbations in the positive and/or negative feedback. Specifically, we consider different oscillatory modulations in the parameters for positive and negative feedback and investigate their effect on the evolution of the system and Probability Density Functions (PDFs). Depending on the relative time scale of the perturbation to the response time of the system (the linear growth rate), we demonstrate the maintenance of the initial condition for a long time, manifested by a broad bimodal PDF. We present the analysis of Fisher information in different cases and elucidate its implications for the sustainability of population dynamics. We also show that a purely oscillatory growth rate can lead to a finite amplitude solution while self-organisation of these systems can break down with an exponentially growing solution due to the periodic fluctuations in negative feedback.

Keywords: Nonlinear system, Sustainability, Fisher Information, Driving parameters, Probability Density Function(PDF).

1 Introduction

Nonlinear dynamical systems have been widely used as simple models for complex phenomena, e.g. in environmental, astrophysical and geophysical, and biological systems. In particular, the utility of such models in understanding biosystems has grown significantly in recent years as ever-improved experimental data has become available. A logistic model, first proposed by Verhults to describe the growth of human populations in 1838 (see [1, 2]), is one of the most popular models for the growth in biological systems, e.g. bacteria, tumor cells, etc (see e.g. [3] and references therein). As a mean field equation, the logistic model describes the time-evolution of macroscopic (large-scale) variables where the overall effect of micro-scale (small-scale) variables is incorporated by control parameters for the positive and negative feedback. The merit of this model lies in the simplicity of the incorporation of the two complementary effects of a positive feedback (which drives the growth) and a negative feedback (which regulates its growth), thereby serving the simplest model for a self-regulated system where the growth is regulated within a system. The balance between the positive and negative feedback leads to a stable equilibrium point (the so-called carrying capacity), to which a system stabilizes in a long time limit, regardless of the initial condition. Thus, a unique value of a carrying capacity can be viewed as a loss of the memory of the initial points.

Many researchers have extended the logistic model to include perturbations in the model parameters for feedback by periodic or random modulation (e.g. [4–11]) or to couple the evolution of other systems (e.g. [12]). In particular, the possibility of a bimodal Probability Density Function (PDF) was demonstrated in the presence of a correlation between a multiplicative noise (for the growth rate) and additive noise. The purpose of this paper is to revisit this logistic model in view of the sustainability for different perturbations. We compute PDFs for different modulations in the model parameters and elucidate fundamental mechanisms determining the shape of PDFs. In particular, we demonstrate that when the characteristic time scale associated with the perturbation is much shorter than the system's response time, the system maintains a long-term memory of initial conditions, thereby leading to a broad bimodal distribution. The sustainability of a system in different cases is examined by computing Fisher information averaged over the total time (F_T). To test the stability of the most sustainable state inferred from our analysis of F_T, we add a periodic stimulus to our system and test the resilience of our system to the environmental perturbation, modeled by a periodic **stimulus**.

The influence of fluctuating environments on the growth of cell populations has been studied (see e.g. [13, 14]); more interestingly, the effect of fluctuating parameters have been studied in other dynamical systems (e.g. [15–22]) while the dynamics of such systems has hardly been investigated from the perspective of information theory. Simplicity of the logistic equation enables us to undertake a systematic investigation in this regards. The remainder of the paper is organised as follows. We introduce our model in §2 and present PDFs and Fisher information in §3 and §4, respectively, when the model parameters for both positive and negative feedback have the same periodic fluctuations. In §5, we test the stability of our system by adding a periodic stimulus. Section 6 summarises the results for different types of modulation of the model parameters. Conclusions are provided in §7.

2 Model and Motivation

We consider a population x (> 0) and its logistic equation in the following form:

$$\frac{dx}{dt} = Nx\left(1 - \frac{x}{K}\right). \tag{1}$$

Here, N is the net growth rate, and K (> 0) is the carrying capacity of the system representing the maximum population size that can be supported by the system. While x can represent the population of any species of interest (e.g. tumor, rabbit, bacteria, etc). In this paper, we consider x to be the population of bacteria to be specific unless stated otherwise. The linear term Nx with $N > 0$ represents a positive feedback bf such as the net effect of bacteria growth (e.g. by eating food) and its death (e.g. by nature death, or antibiotics) while the nonlinear term Nx^2/K represents a negative feedback due to the crowding effect as their growth is inhibited by limited resources. We note that regardless of the initial value of $x(t = 0) = x_0$, x reaches the carrying capacity K as $t \to \infty$ for a constant $N > 0$.

Compared to the case when the linear growth rate is constant or contains periodic fluctuations in the absence/presence of a periodic stimulus, it is less well understood what happens when the model parameter for the negative feedback contains periodic fluctuations as would happen when the negative feedback is delayed in time or is heterogeneous. Periodic fluctuations in negative feedback can provide an interesting mathematical model for the decrease in self-regulation, e.g. in biosystems (e.g. [7, 10]). While we comment on the cases where the model parameter for only positive or negative feedback contains periodic fluctuations in §6, of particular interest in this paper is the case where the perturbation in positive and negative feedback is strongly correlated. Specifically, in §2-4, we focus on the case of the following periodic modulation:

$$N = B + N_0 \sin(\omega t), \tag{2}$$

where B is a constant growth while N_0 and ω are the amplitude and frequency of the modulation. The exact solution to Eq. (1) with Eq. (2) is easily found as:

$$x(t) = \frac{-Kx_0 \exp\left(Bt + \frac{N_0}{\omega}(1 - cos(\omega t))\right)}{(x_0 - K) - x_0 \exp\left(Bt + \frac{N_0}{\omega}(1 - cos(\omega t))\right)}, \tag{3}$$

where x_0 is the initial value of x at $t = 0$. From this analytical solution, we can see the cross-over behavior of x between x_0 and K in the limit of $t \to \infty$. For example, when $\omega = 0$, $\cos(\omega t) = 1$ and $B = N_0 = constant$, $x(t)$ tends to the carrying capacity K as $t \to \infty$. On the other hand, when $B = 0$, the net growth rate fluctuates between $|N_0|$ and $-|N_0|$ in time with zero average – specifically, at times when $\cos(\omega t) = 1$, $x(t)$ takes its minimum value $x_{min} = x_0$ while at times when $\cos(\omega t) = -1$, $x(t)$ reaches its maximum value.

$$x_{max} = \frac{Kx_0}{x_0 + (K - x_0)\exp\left(-\frac{2N_0}{\omega}\right)}. \tag{4}$$

$B = 0$ is an interesting case where the killing effect from natural death or antibiotic is quite strong. In population genetics, this case would correspond to the random sampling of **gametes** with no selective advantage (see §6-7 in [23]) if the periodic modulation is replaced by a short-correlated noise. In the following, we focus our analysis on the case $B = 0$. Furthermore, since t and x can always be re-scaled by N_0 and K, respectively, we fix the value of N_0 and K to be $N_0 = 5$ and $K = 10$. Of particular interest is the effect of ω on the response of the logistic system. As shall be shown shortly, one of the consequences of the same periodic fluctuations in positive and negative feedback is the maintenance of an initial condition and bimodal distribution.

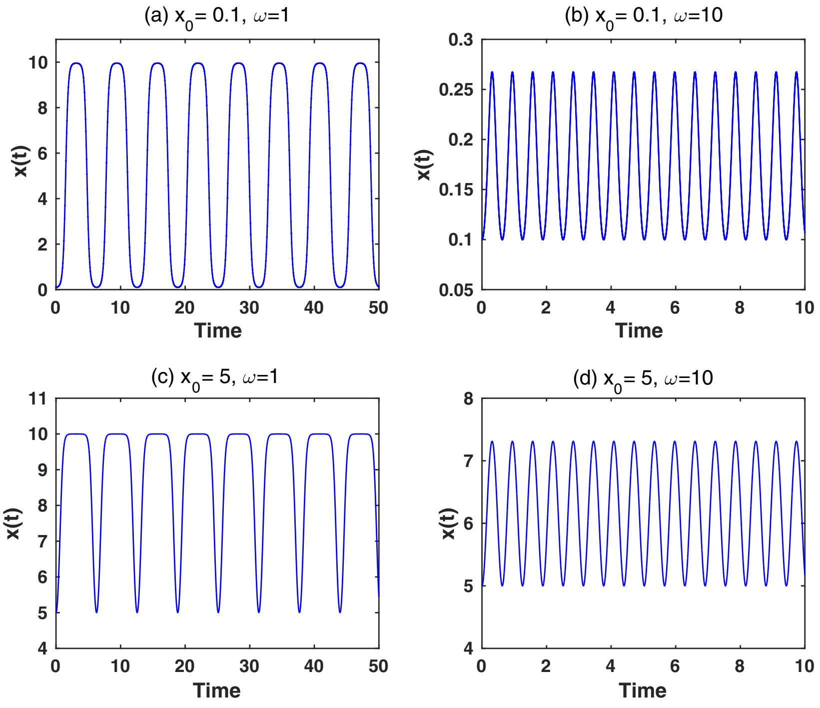

Figure 1: Time trace of $x(t)$ for different values of $x_0 = 0.1, 5$ and $\omega = 1, 10$. For a small value of ω, $x(t)$ tends to reach the carrying capacity $K = 10$ while for large ω, $x(t)$ maintains the initial condition.

In Fig. 1, we first show the typical time history of $x(t)$ for different values of ω and x_0. We first observe that the minimum value of x is equal to x_0, as analytically predicted above. Furthermore, we can confirm that the maximum values in Fig. 1(a)-(d) are the same as Eq. (4). For instance, for $K = 10$, $x_0 = 0.1$, $N_0 = 5$ and $\omega = 10$, Eq. (4) gives $x_{max} = 0.2672$ and this can be seen in Fig. 1(b). For a sufficiently small ω, the time-scale of the perturbation becomes much larger than the system's response time (i.e. the mean square root value of the growth rate), permitting enough time for the population x to reach the carrying capacity regardless of x_0. This means that the bacteria are able to expand as they have enough time to grow during the time when $N > 0$ before decaying when $N < 0$. Mathematically, this is because a fast exponential growth during the time with $N > 0$ wins over the decay during the time with $N < 0$. In comparison, for sufficiently large ω such that the perturbation occurs on time scales much shorter than the growth time, x starting far from $x = x_0 = 10$ can never reach $x = 10$ due to frequent periodic change in N, staying near $x = x_0$ as the bacteria do not have enough time to undergo a substantial exponential growth before they decay. That is, the time interval when $N > 0$ is too short for large ω. As a result, the population of the bacteria fluctuates only near $x = x_0$, never reaching the carrying capacity K.

To demonstrate this cross-over between the case $x \to K$ and $x \to x_0$ for large t in detail, we show the maximum and minimum values of x (in time) for different values of different ω in Fig. 2 (a)-(d). Here, the x-axis represents ω while y shows the maximum and minimum values of x in blue solid line and red dashed lines, respectively. Specifically, Panels (a) and (b) show the maximum and minimum values of x when $x_0 = 0.1$ and $x_0 = 5$, respectively. To highlight the detailed feature for small ω, the same figures in panels (a)-(b) are shown in log-log scale in panels (c)-(d), respectively. From this, we observe a general tendency of the maximum x monotonically decreasing as ω increases.

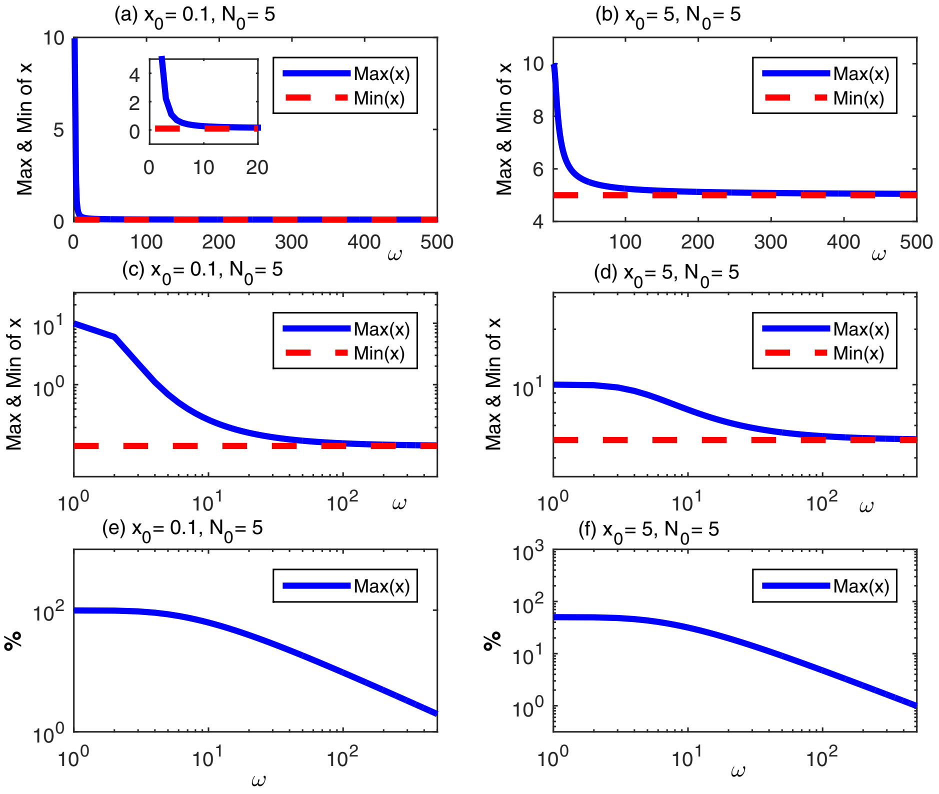

Figure 2: The maximum and minimum values of x as a function of ω for $N_0 = 5$ and $K = 10$ using the initial conditions panels, $x_0 = 0.1$ in panels (a), (c) and (e) and $x_0 = 5$ in panels (b), (d) and (f). (c), (d), (e) and (f) are shown in log-log scales .

We also observe that the minimum of x approximately equals to x_0 in panels (a), (b), (c) and (d) as predicted from the analytical solution. For the maximum value of x, the main difference between the two cases with $x_0 = 0.1$ and $x_0 = 5$ is a much steeper decrease in the maximum $x(t)$ for $x_0 = 0.1$ than for $x_0 = 5$. As the maximum value of $x(t)$ is obtained by the approach to the carrying capacity, the steep drop in the maximum $x(t)$ represents the inability of the system to grow and reach this carrying capacity when the control parameter changes too rapidly in time for higher values of ω, as noted previously. In this case, $x(t)$ does not deviate far from its initial value, effectively leading to the maintenance of the memory of its initial value. This is consistent with the results shown in Fig. 1. To strengthen this argument, we utilise the measure of relative deviation of the maximum values of x to quantify the maintenance of initial conditions. Specifically, we compute the ratio of the change in the maximum of x as follows:

$$\left(\frac{\textbf{Initial value} - \textbf{Maximum of } x}{\textbf{Maximum of } x}\right) \times 100\%. \tag{5}$$

The results are shown in Fig. 2(e)-(f) by using log-log scales. For sufficiently large $\omega \gg 1$, we observe almost straight lines in Fig. 2(e)-(f), suggesting that the percentage change decreases with ω as a power-law in both cases.

3 Probability Density Function

We now examine the effect of ω and x_0 on Probability density functions (PDFs). To this end, we compute the PDF of x by relating the probability of observing the system at a particular value of x to the amount of time the system state spends at x (see [17, 18, 24]) through conservation of the probability:

$$p[x]\ dx = p[t]\ dt. \tag{6}$$

Since t is a continuous variable with a uniform probability density:

$$p[t] = constant = A, \tag{7}$$

we can obtain PDF of x from Eqs. (6)-(7) as:

$$p[x] = p[t]\left|\frac{dt}{dx}\right| = A\left|\frac{dt}{dx}\right| = \frac{A}{u}, \tag{8}$$

where

$$u = \frac{dx}{dt}. \tag{9}$$

Since u is simply given by Eqs. (1)-(2), we can express $p[x]$ in Eq. (8) as

$$p[x] = \frac{A}{(B + N_0 \sin(\omega t))x\left(1 - \frac{x}{K}\right)}. \tag{10}$$

Since Eq. (10) involves the time-dependent function $\sin \omega t$, we need to use Eq. (3) to replace it by a function which only depends on x. To this end, we solve Eq. (3) for $\cos \omega t$ to obtain

$$\cos(\omega t) = 1 + \frac{\omega}{N_0} \ln\left[\frac{x_0(x - K)}{x(x_0 - K)}\right], \tag{11}$$

and then obtain $\sin(\omega t)$ in Eq. (10) from Eq. (11) by using the identity $\left(\sin(\omega t) = \sqrt{1 - \cos^2(\omega t)}\right)$. The PDFs of x ($p(x)$) are shown for different values of ω in Fig. 3.

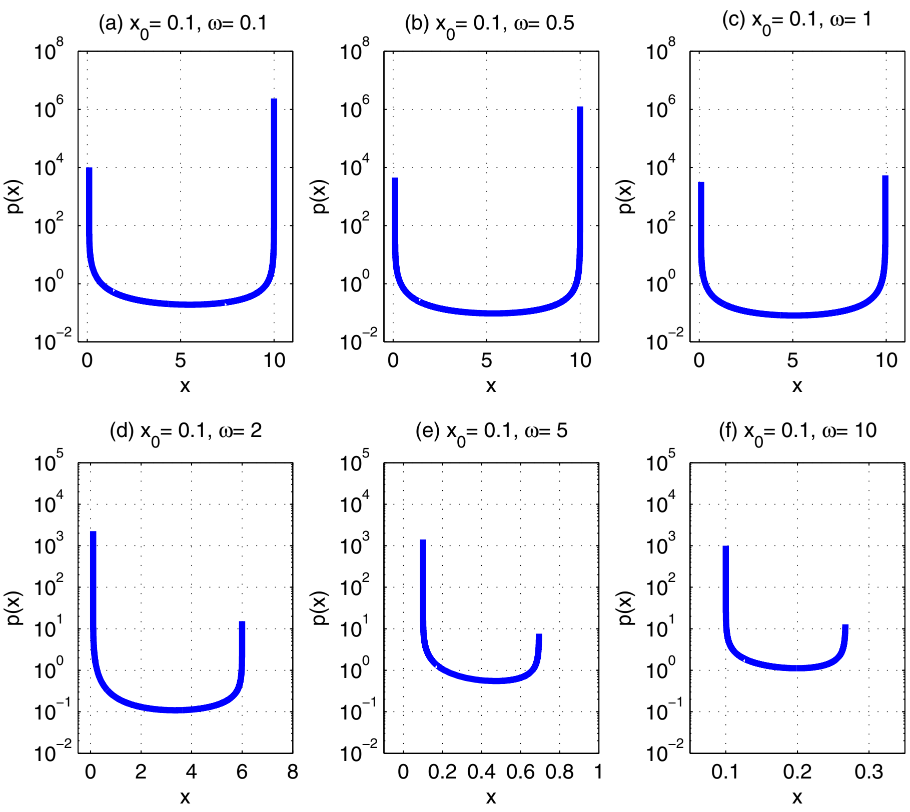

Figure 3: PDF of $x(t)$ for $N_0 = 5$, $K = 10$, $x_0 = 0.1$. Different values of $\omega = 0.1, 0.5, 1, 2, 5, 10$ are used in panels (a)-(f). A bimodal PDF is observed for all the cases.

In Fig. 3, we observe a bimodal PDF for all the cases with different distance between the two peaks. This bimodal distribution results from the maintenance of the initial condition $x_0 = 0.1$ against the tendency of x approaching a carrying capacity ($10 = K$), as noted previously. Specifically, for small $\omega \ll N_0/2\pi$ where the time-scale of the perturbation is much larger than the growth time $1/N$, x reaches the carrying capacity, regardless of x_0, leading to the two peaks at $x = 0.1$ (initial condition) and $x = 10$ ($= K$ the carrying capacity). In comparison, for sufficiently large $\omega \gg N_0/2\pi$, such that the perturbation occurs on time scales much shorter than the growth time (in root mean square value), x starting far from $x = 10$ can never reach $x = 10$ due to frequent periodic change in N, leading to the formation of a very narrow distribution near $x = x_0$. This narrow PDF near x_0 manifests the maintenance of the initial condition when the perturbation occurs much faster than the system's response time. Between these two extreme cases, the bimodal PDF with the largest distance between the two PDF peaks appears for the parameter $N_0/\omega = 5$. It is interesting to observe the gradual shift of the population from the right PDF peak to the left PDF peak with the increase in ω, followed by the narrowing of the PDF. That is, the narrowing of the PDF occurs after the left PDF peak around $x_0 = 0.1$ has grown taller than the right PDF peak.

To demonstrate how the PDF depends on x_0, we show another case in Fig. 4 by using the initial value $x_0 = 5$ much closer to the carrying capacity. Similarly to the case $x_0 = 0.1$ in Fig. 3, Fig. 4 for $x_0 = 5$ demonstrates a bimodal PDF for all cases; for small ω, x reaches the carrying capacity while for large ω, x starting far from $x = 10$ can never reach $x = 10$ and only fluctuates around $x_0 = 5$. Again the distance between the two peaks shrinks as ω increases. However, in contrast to Fig. 3, there is no significant growth of left PDF peak around $x_0 = 5$ for any ω prior to the narrowing of the PDFs in Fig.4. Narrowing of the PDF occurs while the right PDF peak is still larger than the left PDF peak. Specifically, in Fig. 3(c) just before the narrowing of the PDF, the height of the left peak is about [99.9981]% of the height of the right peak while in Fig. 4(b), the height of the left peak is only [49.6632] % of the right peak.

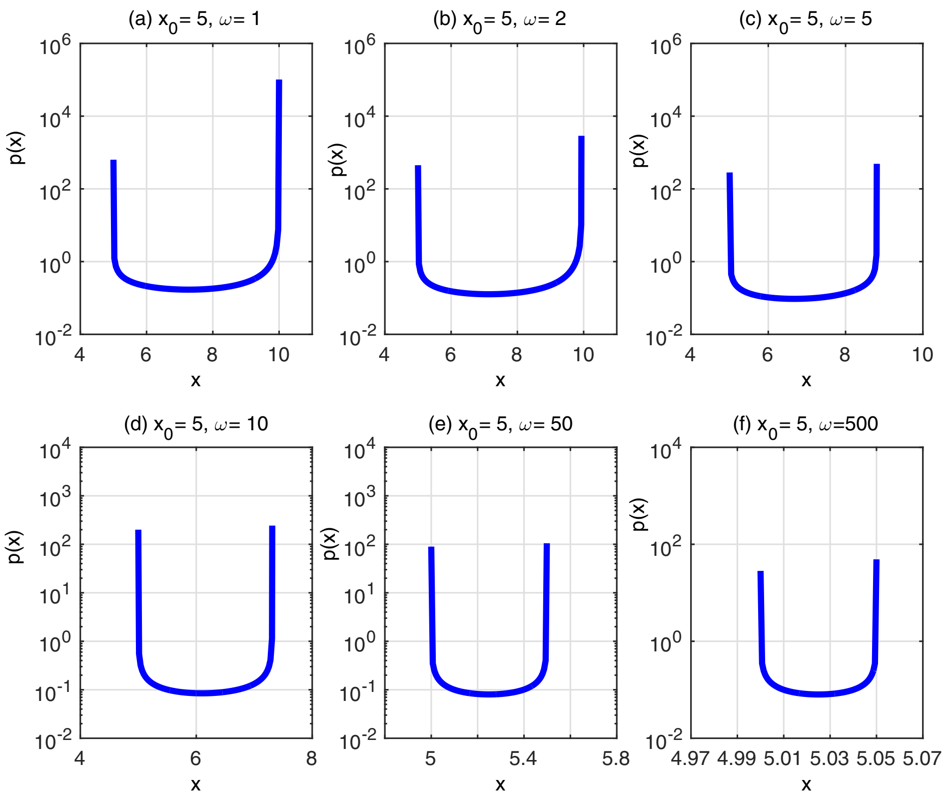

Figure 4: PDF of $x(t)$ for $N_0 = 5$ and $x_0 = 5$ by using different values of ω in panels (a)-(f).

The aforementioned difference in PDFs with $x_0 = 0.1$ and $x_0 = 5$ essentially arises from the fact that the PDF $p[x]$ takes very large value around $x = 0$ and $x = K$. Specifically, Eq. (10) blows up at $x = 0$ and $x = 10$, which respectively correspond to the unstable and stable fixed points of the logistic equation in the case of a constant N. Thus, the nearer x_0 is to $x = 0$, the higher the left peak around x_0, as seen in the case of $x_0 = 0.1$. When x_0 is far from $x = 0$ (as in the case of $x_0 = 5$), the PDF does not form such a high peak around x_0.

As shall be shown below, this has the following interesting consequence in Fisher information. For the initial condition $x_0 = 0.1$ (much less than the carrying capacity), there is an optimal value of ω (satisfying $N_0/\omega = 5$), which can maintain the distinct bimodal PDF with the largest distance between the two PDF peaks while for the initial condition $x_0 = 5$ (closer to the carrying capacity), such an optimal value of ω does not exist because the peak at $x_0 = 5$ is not significant, as noted above. The implication of the existence of such an optimal value of ω will later be related to the utility of Fisher information as a measure of the sustainability.

4 Fisher Information

Results shown in the previous sections highlight a significant change to the logistic model due to periodic modulation in model parameters. In this section, we examine this effect from the point view of Fisher information. Fisher information is a function of the variability (order) of the observations such that low variability (strong order) leads to high Fisher information. That is, a PDF bias to particular x values has higher Fisher information whereas high variability (low order) with a lack of predictability of values of x leads to small Fisher information (e.g. “unbiased” PDF). This is demonstrated in Fig. 5. Previous work suggested the following sustainability hypothesis: *“sustainable systems do not lose or gain Fisher information over time”* [18, 24, 25].

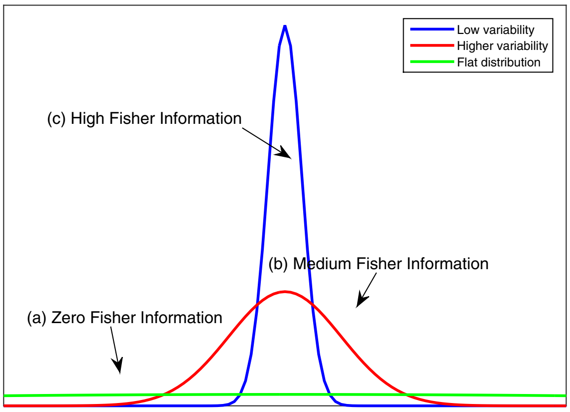

Figure 5: (a) a uniform PDF with zero Fisher information, (b) a PDF of x with a smaller Fisher information and (c) A steeply sloped PDF of x with a large Fisher information (High gradients).

One of the utilities of the Fisher information measure has been in the development of the basic theory of sustainability, for instance, in order to determine whether a system is sustainable or not in diverse physical systems (see [24, 26], [27] and references therein). We recall that Fisher information is a very special uncertainty measure; in contrast to a global measure of uncertainty (e.g., variance, or Shannon’s entropy), Fisher information strongly depends on the gradient of the PDF, consequently, it is sensitive to the local oscillatory character of the PDF and relabeling [20, 27, 28].

By following Cabezac and Fath [18], for a single variable x, Fisher information is calculated from the PDF of x, $p(x,t)$, as follows:[1]

$$F_T = \int \frac{1}{p(x)} \left(\frac{\partial p(x)}{\partial x} \right)^2 dx. \tag{12}$$

We compute the time averaged Fisher information (F_T) by using Eqs. (8), (9) together with

$$\frac{\partial p[x]}{\partial t} = -\frac{A}{u^2} \frac{du}{dt},$$

in Eq. (12) as follows:

$$F_T = \frac{A}{T} \int_0^T \frac{1}{(u(t))^4} \left(\frac{du}{dt} \right)^2 dt = \frac{1}{T} \int_0^T \frac{1}{A} \left(\frac{\partial p(x)}{\partial t} \right)^2 dt. \tag{13}$$

Here, F_T is the Fisher information averaged over the total time duration T. A is a normalization constant. In the following, we investigate the sustainability/variability of our system by computing F_T for different cases. We use the same values of $N_0 = 5$ and $K = 10$, as before, and present F_T for different values of ω and for the two initial values of x, $x_0 = 0.1$ and 5.

For each case with the fixed parameter/initial values (ω and x_0), we compute F_T by varying the total time duration T, for instance, by using $t = [0, 10]$ with $T = 10$, $t = [0, 20]$ with $T = 20$, and so forth

---

[1] We note that Eq. (12) can be extended to n-dimensional system.

and present F_T as a function of T. Fig. 6 shows F_T against T for different $\omega = 0.1, 0.5, 1, 2, 5, 10$ in panels (a)-(f) for the fixed $x_0 = 0.1$, corresponding to the case shown in Fig. 3. Specifically, we use 1000 data points for each panel for $T = 10n$ ($n = 1, 2, 3, ..., 1000$). In each panel, we observe that F_T initially undergoes transient state and approaches an asymptotic value for a sufficiently large T. The higher asymptotic value of Fisher information can be observed for $\omega = 1$ while a small value is observed for $\omega = 0.1$. We show how this asymptotic value of Fisher information varies with ω in Fig. 7. A notable feature of Fig. 7 is the presence of a distinct maximum of Fisher information around $\omega \sim 1$, and this is related to the existence of the optimal ω which maintains the two well-separated peaks in the bimodal PDFs, discussed in relation to Fig. 3.

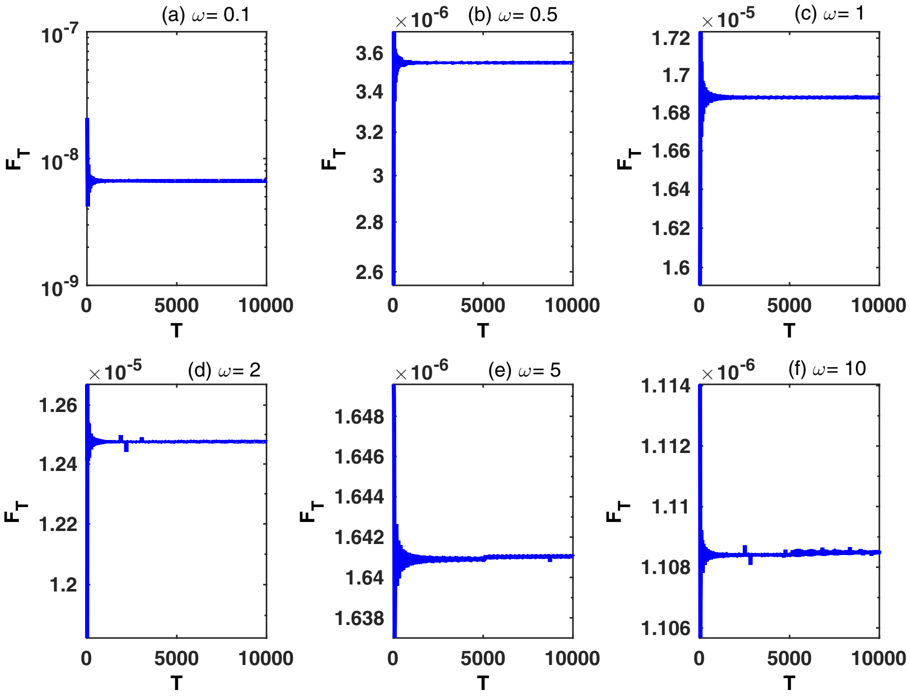

Figure 6: F_T against the total time T for $N_0 = 5$, $x_0 = 0.1$, $K = 10$. Panels (a)-(f) are different values of ω. We can observe the higher value of Fisher information is when $\omega = 1$.

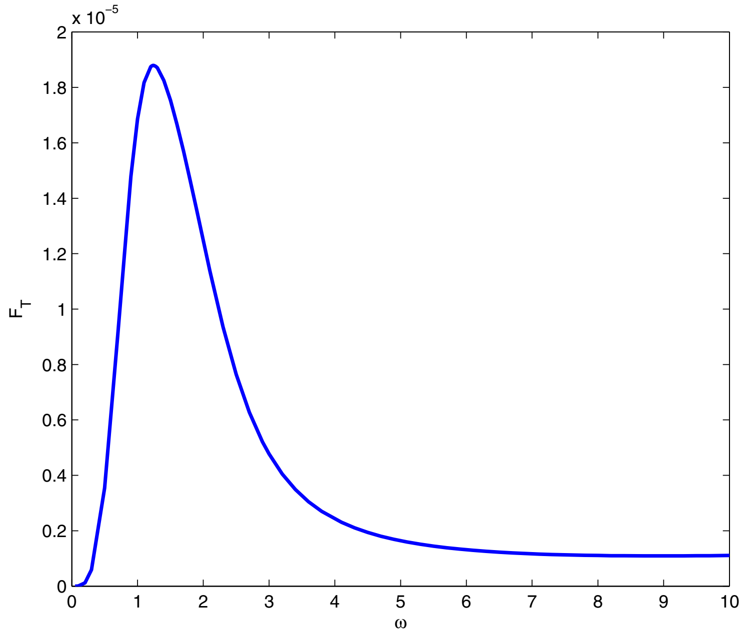

Figure 7: Asymptotic value of F_T against ω for $x_0 = 0.1$.

In the following, this distinct maximum in Fisher information is shown to disappear in the case of $x_0 = 5$, the case corresponding to Fig. 4.

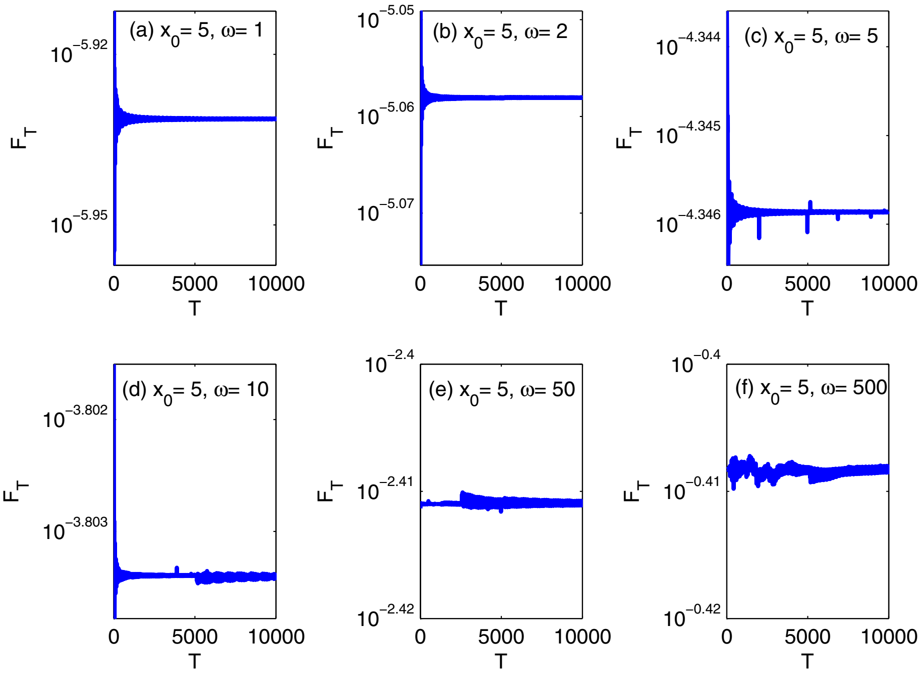

Figure 8: F_T for $N_0 = 5$, $K = 10$ and $x_0 = 5$. Panels (a)-(f) are for different values of ω.

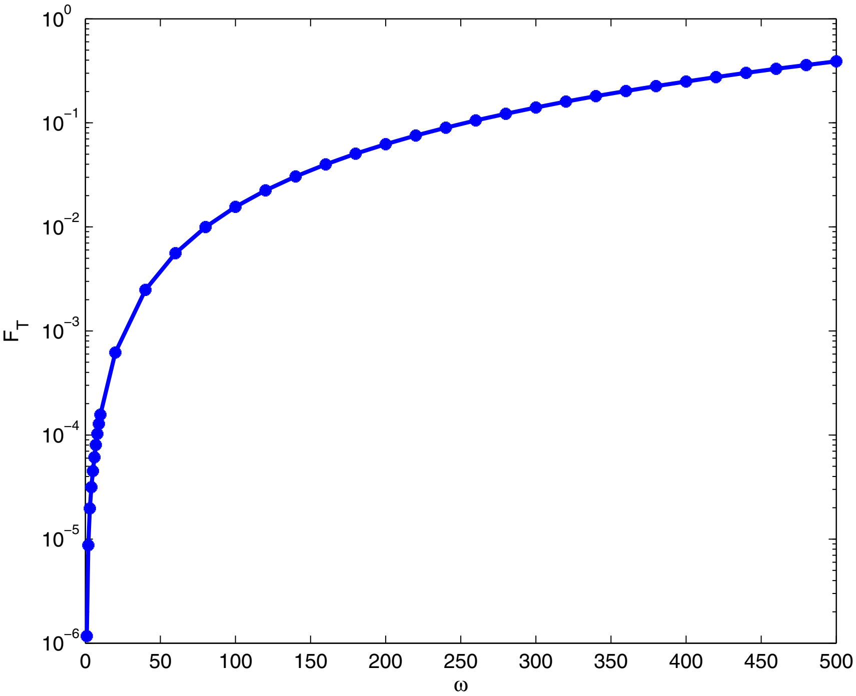

Figure 9: Asymptotic value of F_T against ω for $x_0 = 5$.

Figs. 8 and 9 show F_T against T for different values of ω and the asymptotic value of F_T against ω, respectively, for $x_0 = 5$. Of note is the monotonic increase of Fisher information in Fig. 9, in a sharp contrast to Fig. 7 where we observe the smaller value of Fisher information is at $\omega = 1$, such that higher value appears at $\omega = 500$. This means that we can note a general tendency of Fisher information monotonically increasing as ω increases. This represents that an optimal ω, which maximise Fisher information as in the case where $x_0 = 0.1$, does not exist in this case when $x_0 = 5$ and this is linked to the lack of the two distinct peaks in bimodal PDFs for $x_0 = 5$, as discussed previously in relation to Fig. 4.

5 Role of Fisher Information as a measure of sustainability

In previous sections we found that F_T takes its maximum value around the optimal value of $\omega \sim N_0/5 = 1$ when $x_0 = 0.1$ and $B = 0$. In order to test the sustainability of the optimal case with the maximum F_T, we examine the stability of this optimal case by adding a periodic stimulus $B_1 sin(\omega_1 t)$ as follows:

$$\frac{dx}{dt} = (B + N_0 \sin(\omega t))x\left(1 - \frac{x}{K}\right) + B_1 sin(\omega_1 t), \tag{14}$$

and comparing results with those obtained in non-optimal cases (e.g. $\omega = 10$). We have explored different values of ω, B_1 and ω_1 and in the following, present the results for $\omega = 1$ (optimal case), $\omega = 10$ (non-optimal case), $B_1 = 1, 10$, $\omega_1 = 1, \sqrt{2}$ as example.

First, in Fig. 10, we show how PDFs are affected by different periodic stimulus for $\omega = 1$ in left panels and $\omega = 10$ in right panels. In comparison with the PDFs in Fig. 3(c) and 3(f), respectively, we see that the overall change in PDFs is much less in the optimal case ($\omega = 1$), suggesting that the optimal case with a large Fisher information is less affected by the periodic stimulus than in the non-optimal case. To

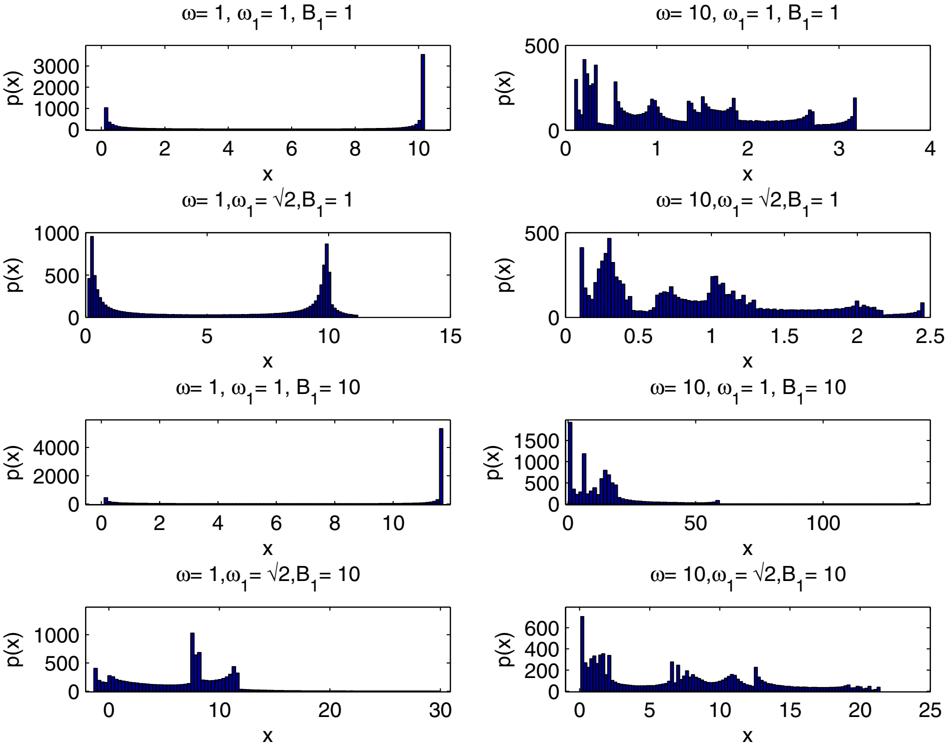

Figure 10: PDF of x for $x_0 = 0.1$ and $N_0 = 5$, with periodic stimulus. Left panels are for the optimal case ($\omega = 1$) while right panels are for the non-optimal case ($\omega = 10$). The PDFs with optimal value $N_0 = 5\omega$ in left panels are more resilient to the periodic stimulus than the PDFs for $\omega = 10$.

strengthen this argument, we utilise the mean value as another measure to quantify the change of the system. Specifically, we compute the mean value without periodic stimulus (shown in Table 1) and the mean value after adding the periodic stimulus, and quantify the ratio of the change in the mean value as follows:

$$\frac{\textbf{Mean value without periodic stimulus} - \textbf{Mean value with periodic stimulus}}{\textbf{Mean value without periodic stimulus}} \times 100\%. \tag{15}$$

The results are shown in Table 2. We can see that in the optimal case $\omega = 1$, the ratio of change in the mean value for different periodic stimulus is much less than that in the non-optimal case ($\omega = 10$). For example, when the parameters in the periodic stimulus have values $B_1 = 1, \omega_1 = 1$, the ratio of change in the optimal case is 15.3% while it is 656.1% in the non-optimal case. This means the ratio of change in the non-optimal case is roughly 44 times bigger than the ratio of change in the optimal case. Thus, the optimal case is more resilient to the perturbation and thus more sustainable compared to non-optimal case.

To complete our investigation on the implication of Fisher information for sustainability, we have also performed similar experiments for $x_0 = 5$ by adding a periodic stimulus of different amplitude and frequencies, and have found no obvious link between the value of F_T and sustainability as there isn't any particular value of ω which is most resilient to perturbation (results are not shown). This is due to the lack of maximum in Fisher information for this initial condition. From these, we propose that the F_T is a useful measure in the case when the Fisher information has a distinct maximum (related to the presence of the two distinct bimodal PDF peaks).

Mean value in optimal case	Mean value in non-optimal case
5.5433	0.1733

Table 1: Mean value in the optimal and non-optimal cases without periodic stimulus; $x_0 = 0.1$

	Optimal case		Non-optimal case	
	Mean value	% Change (11)	Mean value	% Change (11)
$B_1 = 1, \omega_1 = 1$	6.3927	15.3 %	1.3103	656.1 %
$B_1 = 1, \omega_1 = \sqrt{2}$	5.5515	0.2 %	0.8814	408.6 %
$B_1 = 10, \omega_1 = 1$	8.8326	59.3 %	15.2631	8707.3 %
$B_1 = 10, \omega_1 = \sqrt{2}$	6.5509	18.2 %	7.2068	4058.6 %

Table 2: % change in mean value in the optimal and non-optimal cases with periodic stimulus; $x_0 = 0.1$

6 Comments on different modulation

We have so far focused on the case where the same periodic modulation is applied to both positive and negative feedbacks. To complete our investigation, we now comment on the effect of the two different modulations.

6.1 Case-1: Perturbation in the positive feedback

We consider a periodic modulation in the parameter for the positive feedback and a constant model parameter in the negative feedback. Specifically, we consider:

$$\frac{dx}{dt} = [B + N_0 \sin(\omega t)]x - \frac{Cx^2}{K}, \tag{16}$$

where the values of B, C, and K are kept constant. In Fig. 11, we illustrate the effect of different values of ω and N_0 on PDFs for $B = 0$, $K = 10$, $C = 1$, and $x_0 = 0.1$. By taking $B = 0$, we are again modeling the case where the growth is strongly inhibited and is driven only by periodic fluctuations. Even when the linear growth rate has zero average, we observe the excitation of the finite amplitude solution, similar to the result in [10]. This finite amplitude solution leads to PDFs centered around the initial position $x_0 = 0.1$ with a single peak, as shown in Fig. 11. That is, in contrast to the bimodal PDFs in the previous sections, we observe a unimodal PDF in all cases. This reflects the main effect of periodic fluctuations in driving a unimodal PDF. The width of PDFs near $x = x_0$ becomes narrower as ω increases, similarly to the behaviour of the bimodal PDFs in the previous sections.

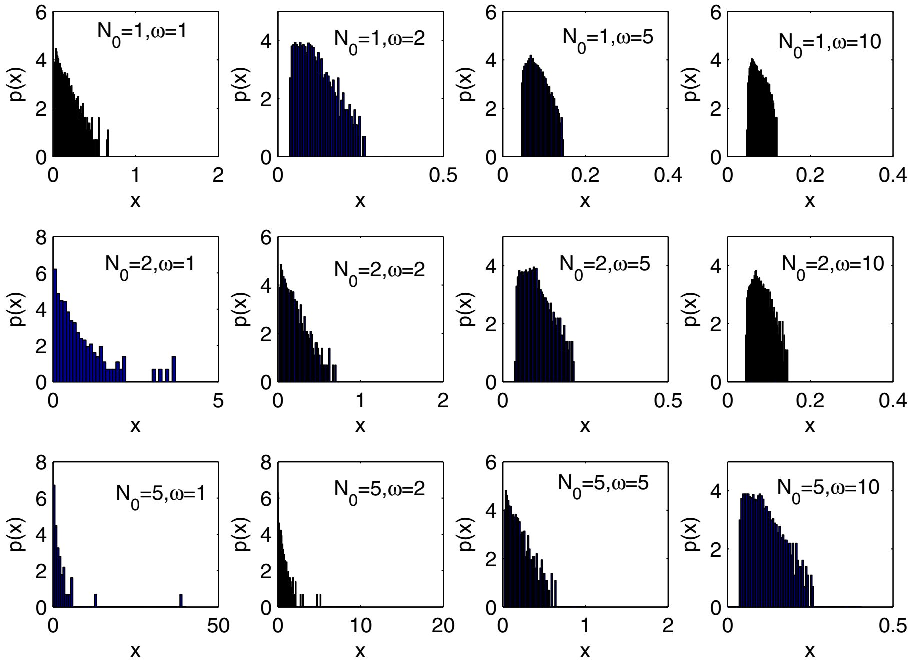

Figure 11: PDFs of x for Case-1 for different N_0 and ω. $x_0 = 0.1, B = 0, K = 10, C = 1$. We observe a notable unimodal PDFs for all the cases.

6.2 Case-2: Perturbation in the negative feedback

We finally consider that case where a periodic fluctuations in the parameter are included only in the negative feedback as follows:

$$\frac{dx}{dt} = Cx - \frac{[B + N_0 \sin(\omega t)]x^2}{K}. \tag{17}$$

The analytical solution to Eq. (17) can be found as:

$$x = \frac{KabCx_0}{KCa + N_0Cbx_0c + N_0C\omega x_0 + Bx_0a(b-1)}, \tag{18}$$

where

$$a = C^2 + \omega^2,$$

$$b = \exp(Ct),$$

$$c = C\sin(\omega t) - \omega\cos(\omega t).$$

As the amplitude of N_0 relative to B increases, the solution starts growing exponentially as the nonlinear damping becomes ineffective (e.g. [7, 10]).

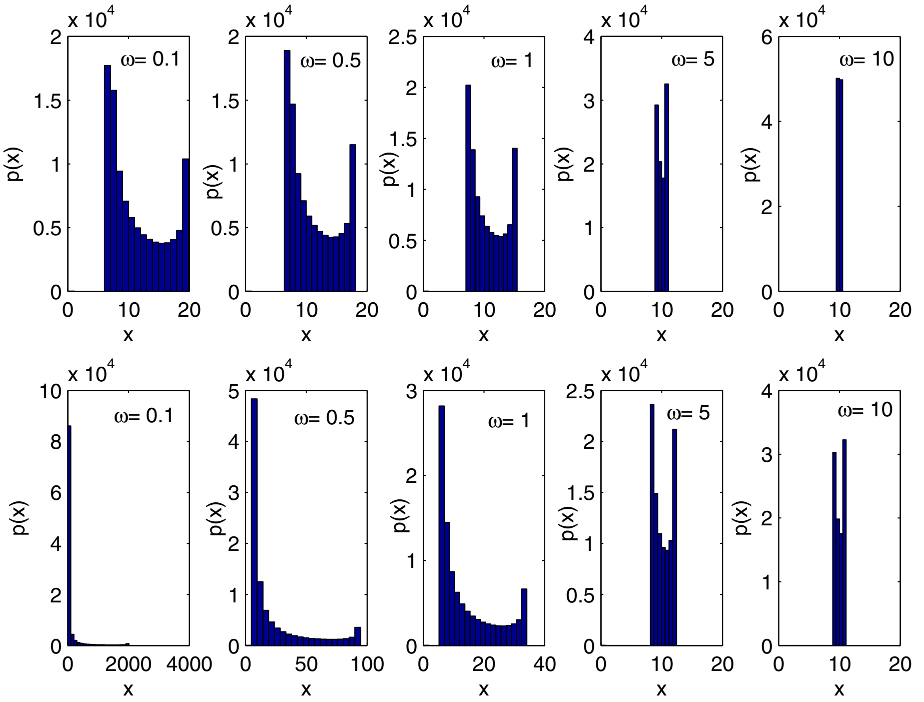

Figure 12: PDFs of x for two different $N_0 = 0.5$ and 1 in the upper and lower panels, respectively. For all cases, $x_0 = 0.1$, $B = 1$, $K = 10$, and $C = 1$, PDFs are biomodal.

The resulting PDFs are shown in Fig. 12 for $N_0 = 0.5$ in the upper panels and $N_0 = 1$ in the lower panels, respectively, for the same $x_0 = 0.1$, $B = 1$, $K = 10$, and $C = 1$. We observe that when $N_0 = 1$, the PDFs become broader as ω decreases. The broadening of PDFs is related to the strong intermittency of x, manifested by the high-amplitude peaks as ω decreases. This can be seen from the time trace in Fig.13. In particular, we note that the solution grows exponentially for sufficiently large N_0 and small ω, as shown in panel (c) for $\omega = 0.1$ and $N_0 = 10$.

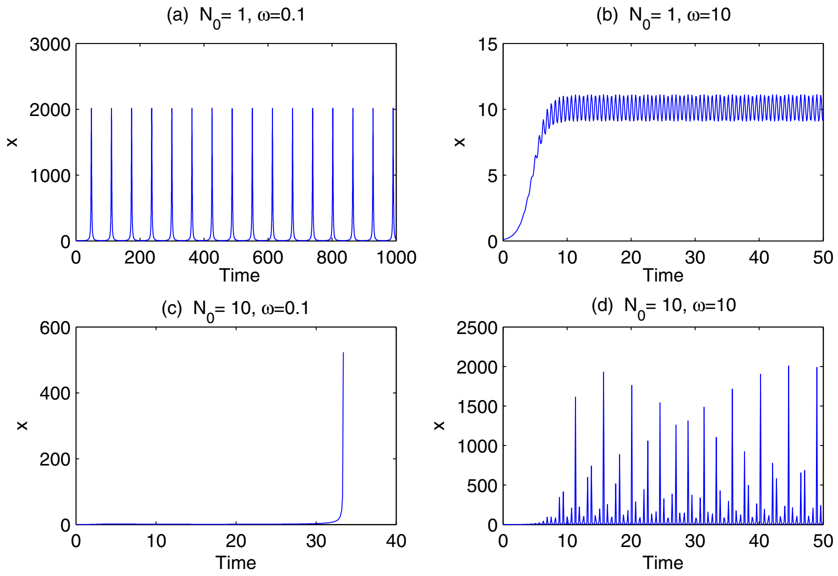

Figure 13: $x(t)$ against t for $N_0 = 1, 10$ and $\omega = 0.1, 10$. For all cases, $x_0 = 0.1$, $K = 10$, $B = 1$, $C = 1$

7 Conclusions and discussion

We have revisited the logistic model in view of sustainability for different perturbations in the model parameters for both positive and/or negative feedback and investigated the effect of different modulations and initial conditions. In particular, we demonstrated the possibility of the maintenance of a long-term memory of initial conditions when the characteristic time scale associated with the disturbance is much shorter than the system's response time, as well as bimodal distributions. In the case of the same periodic modulation of the model parameters for the positive and negative feedback, for the initial condition far from the carrying capacity ($x_0 = 0.1$), we found a distinct maximum value of Fisher Information for an optimal value of parameters $N_0 \sim 5\omega$ due to a broad bimodal PDFs with two distinct peaks. In contrast, for $x_0 = 5$, Fisher Information was shown to monotonically increase with ω, with no distinct maximum. The sustainability of a system under different perturbations is examined by computing F_T from PDFs. In particular, we found that Fisher Information is a useful measure of sustainability in the case when it has a distinct maximum as a consequence of the presence of the two distinct bimodal PDF peaks.

Our results could have interesting implications for understanding the origin of the survival of small populations of bacteria which do not get killed off by antibiotics (or tumour persisted) (e.g. [29]), as manifested by a PDF peak around the small x_0. That is, the initial population of bacteria of small size (corresponding to small x_0 in our model) can survive under the strong antibiotics, maintaining a broad bimodal PDF for an optimal condition with the maximum Fisher Information. Thus, the optimal case has the best survival likelihood. As the optimal perturbation frequency occurs when its time scale is of order of the time scale of the linear growth rate (in root mean square value), it may well be that the population with such growth rate would have the best fitness. Alternatively, this suggests that the best killing efficiency would be achieved by choosing sufficiently large frequency ω above this optimal value. It would be of interest to extend our work to other systems such as a coupled logistic equations and a Gompertzian equation and study their implications in future work.

References

[1] S. Sinha & S. Parthasarathy, "Behaviour of simple population models under ecological processes", J. Biosci., Vol. 19, 2, 247-254, (1994).

[2] J. Loyd, A. Minnich & O. Mondragon, "Project 1: Logistic map and chaotic dynamics", CS 423/523, (2013).

[3] Z. Weirong, SH. Yuanzhi & H. Zhenhui, "Stochastic resonance in the growth of a tumor induced by correlated noises", Chinese Science Bulletin, 50, Issue 20, 2273-2275, (2005).

[4] C-Y. Wang, Y. Gao, X-W. Wang, Y. Song, P. Zhou & H. Yang, "Dynamical properties of a logistic growth model with cross-correlated noises", Physica A 390, 1-7, (2011).

[5] B-Q. Ai, X-J. Wang, G-T. Liu & L-G. Liu, "Correlated noise in a logistic growth model", Phys. Rev. E 67, 022903, (2003).

[6] C-J. Wang, Chinese Phys. B 22, 6060502, (2013).

[7] T. Wright, J. Twaddle, C. Humphries, S. Hayes & E. Kim, "Variability and degradation of homeostasis in self-sustained oscillators", Mathematical Biosciences 273, 57-69, (2016).

[8] C. Lu & X. Ding, "Survival analysis of a non-autonomous logistic model with stochastic perturbation", Journal of Applied Mathematics Vol. 2012, Article ID 692742, (2012).

[9] M. Liu & K. Wang, "Persistence and extinction of a non-autonomous logistic model with random perturbations", Commun. Math. Sci., 10, 3, 977-987, (2012).

[10] U. Lee, J.J. Skinner, J. Reinitz, M.R. Rosner & E. Kim, “Noise-driven phenotypic heterogeneity with finite correlation time in clonal populations”, PLoS ONE 10(7): e0132397, (2015).

[11] I. Prigogine & I. Stengers, “Order out of chaos: Man’s new dialogue with Nature”, United States, (1984).

[12] C. Wang, L. Di & M. Dong-Cheng, “Pure multiplicative noises induced population extinction in an anti-tumor model under immune surveillance”, Commun. Theor. Phys. (Beijing, China) 52, 463467, (2009).

[13] M.K. Belete & G. Balazsi, “Optimality and adaptation of phenotypically cells in fluctuating environments”, Phys. Rev. E 92, 062716, (2015).

[14] M. Thattai & A. Oudenaarden, “Stochastic gene expression in fluctuating environments”, Genetics 167: 523-530, (2004).

[15] M. Mohamed & E. Kim, “Parametric instability and nonlinear feedback in complex lorenz systems”, (2016), under review.

[16] J. Priede, R. Avalos-Zuniga & F. Plunian, “Homopolar oscillating-disc dynamo driven by parametric resonance”, Physics. Letters A 374, 584-587, (2010).

[17] H. Cabezac & B. Fath, “Towards a theory of sustainable systems”, Fluid Phase Equilibria 194-197, 3-14, (2002).

[18] B.D. Fath, H. Cabezas & C.W. Pawlowsk, “Regime changes in ecological systems: an information theory approach”, Journal of Theoretical Biology 222, 517-530, (2003).

[19] M. Mohamed & E. Kim, “Oscillatory control parameters in nonlinear chaotic systems”, Phys. Scr. 89, 1-8, (2014).

[20] Y. Shastri & U. Diwekar, “Sustainable ecosystem management using optimal control theory: Part 2 (Stochastic systems)”, Journal of Theoretical Biology 241, 522-532, (2006).

[21] A.L. Mayer, C.W. Pawlowski, & H. Cabezac, “Fisher information and dynamic regime changes in ecological systems”, ecological modelling 195, 72-82, (2006).

[22] A. Sood & E. Kim, “Dynamic model of dynamo (magnetic activity) and rotation”, A & A 555, A22, (2013).

[23] M. Kimura, “Diffusion models in population genetics”, J. Appl. Prob. 1, 177-232 (1964).

[24] V. Rico-Ramirez, M.A. Reyes-Mendoza, P.A. Quintana-Hernandez & J.A. Ortiz-Cruz, “Fisher information on the performance of dynamic systems”, Ind. Eng. Chem. Res. 49, 1812-1821, (2010).

[25] B.R. Frieden & B.H. Soffer, “Lagrangian’s of physics and the game of Fisher-Information transfer”, The American Physical Society, 52, 3, (1995).

[26] A.M. Gonzalez-Mejia, T. Eason, H. Cabezas & M.T. Suidan, “Computing and interpreting fisher information as a metric of sustainability: regime changes in the United States air quality”, Clean Techn Environ Policy 14:775-788, (2012).

[27] P. Sanchez-Moreno, A.R. Plastino & J.S. Deshesa, “A quantum uncertainty relation based on fishers information”, J. Phys. A: Math.Theor. 44, 065301 (9pp), (2011).

[28] C.W. Pawlowski, B.D. Fath, A.L. Mayer & H. Cabezas, “Towards a sustainability index using information theory”, Energy 30, 1221-1231, (2005).

[29] A. Shalek, et al, “Single-cell transcriptomics reveals bimodality in expression and splicing in immune cells”, Nature 498(7453): 236-240, (2013).